Determination of Parameters of Radiation Induced Traps in Silicon

R.Siemieniec[1], W.Südkamp[2], J.Lutz[3]

[1]Institute of Solid-State Electronics, Technische Universitaet Ilmenau, PO Box 100565, D - 98684 Ilmenau, Germany, Phone: +49 3677 693225, Fax: +49 3677 693777, e-mail: ralf.siemieniec@tu-ilmenau.de

[2]Aktiv Sensor GmbH, Ruhlsdorfer Str.95, Gebäude 4, D-14532 Stahnsdorf, Germany, e-mail: wsuedkamp@aktiv-sensor.de

[3]Faculty of Electrical Engineering and Information Technology, Technical University of Chemnitz, D-09107 Chemnitz, e-mail: josef.lutz@infotech.tu-chemnitz.de

ABSTRACT: Irradiation techniques are nowadays widely used for carrier lifetime adjustment in silicon power devices because of their very good reproducibility. But still there are missing or incomplete recombination center data for use in device simulation. Based on DLTS and lifetime measurements, the center properties of the most important traps after electron irradiation and annealing with a temperature above 330°C are determined in this work within a wide temperature range. These parameters have been used for device simulation of irradiated power diodes and correctly explain the temperature dependencies of forward voltage as well as of switching characteristics.

KEYWORDS: Charge carrier lifetime, Electron Irradiation, Recombination Model, DLTS Measurements, Lifetime Measurements, Capture Coefficients, Device Simulation

1 INTRODUCTION

Radiation induced centers are widely used for carrier lifetime adjustment in modern power devices and replace the conventional impurities gold and platinum because of the possibility of exact process control. Center properties as published in a wide number of papers differ largely. One reason is that the center properties depend on creation conditions and especially on the annealing process after irradiation.

It is necessary to know the parameters of the centers, especially their temperature dependency. Some publications deal with centers in high power devices which are mounted in pressure contact technology [1] whereas most modern power devices are mounted in modules. It must be ensured that a solder process up to >300°C will not change the device parameters. Therefore an annealing step is necessary, and this thermal process changes the composition of these centers. Thus, for instance, divacancies are most likely to vanish. This paper deals with the important traps in silicon after electron irradiation and an annealing process of 1h at >330°C.

The most important trap for recombination in devices undergoing this annealing process is the A-Center E(90K). Its level is far outside of the mid of the bandgap. Earlier publications [2] showed sufficient agreement with the measured reverse recovery charge, but they could not explain the temperature dependency of the forward voltage drop. It is important to achieve a positive temperature coefficient $\Delta V_F/\Delta T$ between 300K and 400K because most modern devices are paralleled inside power modules.

The results of our investigations explain the temperature dependency of the forward voltage as well as the temperature dependency of the dynamic parameters of freewheeling diodes.

2 RECOMBINATION CENTERS AND LIFETIME

2.1 Recombination model

Common device simulation tools offer a simple default recombination model using the well known Shockley-Read-Hall equation as stated in Appendix C. Only one recombination level can be treated by this model under quasi equilibrium conditions [3],[4]. For a trap or recombination center it is assumed that it has an energy level in the band gap and its charge state may have one of two values differing by one electronic charge (eq.1).

$$R_{SRH} = \frac{pn - n_i^2}{\tau_{p0}(n + n_1) + \tau_{n0}(p + p_1)}$$

(1)

Herein the electron and hole concentrations are given by n and p, their product under equilibrium conditions being n_i^2. The minority carrier lifetimes for electrons and holes are determined by τ_{n0} and τ_{p0}, while n_1 and p_1 are the equilibrium carrier concentrations corresponding to the Fermi-level position coincident with the recombination level position in the band gap.

However, this simple model does not include more than one recombination center as well as the trap charging processes which strongly influence the dynamic behavior of the power device. An extended recombination model which includes trap dynamics for coupled defect levels as found after gold or platinum diffusion has been included in the 1D diode simulator ADIOS first [5]. For simulation purposes of irradiated devices, the 2D device simulator TeSCA [6] uses a newly implemented model including the full set of rate equations for independent recombination centers with a single charge state energy level as given in Appendix B. This model allows the simulation of the complete dynamical behavior of a device with more than one recombination level with different recombination parameters under different conditions (Appendix C).

2.2 Lifetime at high- and low-level injection

Carrier lifetime obtained from deep level recombination can be treated by Shockley-Read-Hall (SRH) statistics. Assuming that excess carrier concentrations are equal, the SRH lifetime for a number of independent deep levels is given by eq.2.

In case of low-level injection $\delta n << n_0$ and in n-type silicon $n_0 >> p_0$, eq.2 simplifies to eq.3 which shows that for recombination centers close to the mid of the bandgap the low-level lifetime τ_{LL} is equal to the hole minority carrier lifetime τ_{p0} in this case. Furthermore, low-level lifetime is controlled by traps close to the intrinsic level.

At high-level injection, the excess carrier density is much higher than the equilibrium densities: $\delta n >> n_0, n_1, p_0, p_1$. The high-level lifetime τ_{HL} is given by eq.4. The high-level lifetime does not directly depend on the recombination center position, but on trap concentration and capture coefficients.

$$\frac{1}{\tau_{SRH}} = \sum_{j=1}^{k} \frac{n_0 + p_0 + \delta n}{\tau_{p0j}\left(n_0 + n_{1j} + \delta n\right) + \tau_{n0j}\left(p_0 + p_{1j} + \delta n\right)} \tag{2}$$

$$\frac{1}{\tau_{LL}} = \sum_{j=1}^{k} \frac{n_0}{\tau_{p0j}\left(n_0 + n_{1j}\right) + \tau_{n0j} p_{1j}} \tag{3}$$

$$\frac{1}{\tau_{HL}} = \sum_{j=1}^{k} \frac{1}{\tau_{n0j} + \tau_{p0j}} \tag{4}$$

2.3 Influence of recombination center position

Then recombination center position has a strong influence on the carrier lifetime. In n-type semiconductors, the value of n_1 describes the position of recombination level.

Since high-level injection is found only if excess carrier density δn is much higher than n_1, validity of this approach strongly depends on the value of n_1 which is given by eq.5 (in p-type silicon one has to consider the value of p_1 according to eq.6). If this condition is not met, any measured high-level injection lifetime will apparently depend on excess carrier density.

Furthermore, the value of n_1 not only depends on recombination center position but of course also on temperature.

In case of low-level injection, the low-level lifetime is sensitive to small changes of background doping if the value of n_1 is somewhere in the region of the value of equilibrium carrier density n_0.

$$n_1 = n_i \exp\left(\frac{E_T - E_I}{k_B T}\right) \tag{5}$$

$$p_1 = n_i \exp\left(\frac{E_I - E_T}{k_B T}\right) \tag{6}$$

2.4 Influence of temperature

Temperature dependence of lifetime is different at low-level and high-level injection. At high-level injection, the temperature dependence of lifetime is determined by the temperature dependencies of the capture coefficients. If the capture coefficients for electrons and holes clearly differ, the smaller one controls temperature dependence of the high-level lifetime.

At low-level injection, the temperature dependence of carrier lifetime is also influenced by the temperature dependence of the quantities n_1 and p_1 – both of them increase with increasing temperature.

3 DEVICE PREPARATION

Diode samples were prepared using the Semikron CAL-diode (CAL: Controlled Axial Lifetime) production line on neutron transmutation doped float zone silicon wafers. The devices have a pin-structure with a wide nn^+-junction, the pn-junction depth is approximately 20µm. The base width of all samples is about 90µm at a doping concentration of $6 \cdot 10^{13} \, cm^{-3}$. All devices have an active area of $6mm^2$ and were annealed at over 330°C for one hour. The nominal rated current is about 10A ($166A/cm^2$), the blocking voltage is 1200V.

For measurement purposes, electron irradiation at an energy of 1.1MeV was applied with different doses as shown in table 1. Sample N is used for the characterization of the base silicon properties and has undergone no lifetime adjustment steps. For optical excitation of excess carriers a hole with an diameter of 1.8mm is etched into the anode metallization.

The sample PE is based on $3 \cdot 10^{13} \, cm^{-3}$ p-type Silicon and is used for DLTS measurement purposes.

4 MEASUREMENT TECHNIQUES

4.1 DLTS Measurement Principle

With Deep Level Transient Spectroscopy (DLTS), pulsed base capacitance transients of a pn-junction with deep levels are analyzed as a function of temperature [7]. During a fill-pulse, deep levels are filled with charged carriers and during the reverse phase, the deep levels are discharged by thermal emission, creating an exponential capacitance transient. The transient is sampled at two time points t_1, t_2 and their difference - the DLTS signal - is recorded as a function of temperature. If the rate window $(t_2-t_1)/\ln(t_2/t_1)$ corresponds to the emission time constant, the DLTS signal reaches a maximum. The intensity of these DLTS peaks are proportional to the trap density. To obtain the most important trap parameters energy level and the range of capture cross section, an arrhenius plot is constructed by variation of the rate window for a trap. However, in most cases the capture cross section must be measured directly by variation of the fill-pulse duration because of the entropy factor and temperature dependence of the capture cross section.

4.2 OCVD Measurements

The Open Circuit Voltage Decay (OCVD) method was introduced in 1955 [8]. A steady-state excess carrier concentration is applied by a forward current flow through a diode (fig.1a). After an abrupt opening of the circuit at t=0, recombination of excess carriers will take place and the diode's open voltage is monitored (fig.1b). The initial voltage step at t=0 is due to the voltage drop V_0 in the diode, which is observed when the current flow stops. This voltage drop may be used to determine the series resistance of the device. The large drop in the V(t)-curve near t=0 is caused by emitter recombination. This effect becomes negligible for t > $2.5\tau_b$, where τ_b is the base lifetime [9]. It is possible to estimate the carrier lifetime from the linear parts of the slope. For diodes with a pin-structure, as used in these investigations, the lifetime under high injection condition (high-level lifetime) is given by eq.7, whilst the low-level lifetime is given by eq.8 [10]. In case of low-level lifetime measurements one has to

avoid parasitic elements such as capacities and shunt resistances of the measurement setup because their influence on the measurement results due to the low carrier concentrations. The validity of the measurement result depends on the charge stored inside the sample in comparison with the value of external parasitics, if necessary one has to use compensation techniques as described in [11]. The excess carrier concentration in the low-doped base region may be calculated approximately by use of eq.9.

$$\tau_{HL} = \frac{2k_B T}{q} \left(\frac{dV}{dt} \right)^{-1} \tag{7}$$

$$\tau_{LL} = \frac{k_B T}{q} \left(\frac{dV}{dt} \right)^{-1} \tag{8}$$

$$\overline{p} = n_i \cdot \exp\left(\frac{V(t)}{\frac{2k_B T}{q}} \right) \tag{9}$$

According to section 2.3, the necessary excess carrier concentration depends on recombination center position and temperature. In case of comparatively shallow recombination level positions, it is important to generate excess carriers by optical generation of free carriers since it is not possible to realize the required excess carrier generation by the common electrical forward biasing of the sample. For these measurements, the primary wavelength of 1064nm of a pulsed Yttrium-Aluminum-Garnet (YAG) laser is used to generate excess carriers. At this wavelength, the absorption coefficient is approximately 10cm^{-1} [12],[13].

For these measurements we used the diode-pumped, Q-switched YAG Laser JOL-R60 manufactured by JENOPTIK Germany [14]. The laser pulse width was about 100ns with a pulse energy of 6mJ, the pulse frequency was 3kHz while the duration of one pulse sequence

was about 1ms. To realize a homogeneous excitation over the whole device area the laser beam has been defocused.

4.3 Accuracy of Measurements

In this work, the determination of the center concentration is most important since it is used for the capture rate calculation and results in a total error of 10-20% in dependence of the trap concentration. The largest possible error source originates from the determination of the active area of the pn-junction - the square of the area is taken into account for the calculation of doping concentration and therefore center concentration.

The error for activation energy determination depends mostly on the temperature measurement of the sample and is in the range below 10% [15].

The accuracy of the OCVD measurement itself depends on the preciseness of the oscilloscope, the temperature measurement and interfered noise. The total error of the estimated lifetime is lower than 10%.

5 RESULTS

5.1 Non-irradiated samples

Without considering the traps in non-irradiated silicon, no explanation of the behavior of the irradiated samples was possible. Therefore the traps in sample N were investigated.

To begin, the trap properties were determined by DLTS in sample N. Capture coefficients were measured directly by variation of the fill-pulse duration. Table 2 shows all determined center properties. The temperature dependence of the capture cross sections is fitted by use of eq.10. Positive values of E_σ signify a decrease of the capture cross section with temperature, whereas a negative value stands for an increase with temperature.

$$\sigma = \sigma_0 \exp\left(\frac{E_\sigma}{\frac{k_B T}{q}}\right) \qquad (10)$$

In case of E(270K) two contributions are found in trap kinetics. The fraction of the fast part in comparison to the total concentration is about 0.35. According to the DLTS data the high-level lifetime is extrapolated to a temperature of T=300K as shown in the last column of table 2. Obviously, the fast part of E(270K) dominates lifetime in our non-irradiated samples. Nevertheless, exact measurements of the fast parts electron capture coefficients were impossible. The fast part cannot be seen since the minimal pulse width of the DLTS measurement setup is 10ns. Thus, it is only possible to give the order of magnitude for this capture coefficient. Further, it was not possible to measure the hole capture coefficient.

Thus, lifetime measurements offer the possibility for an approximate determination of the capture coefficients. Using OCVD measurements for determination of low-injection lifetime, the hole capture coefficient is calculated by means of eq.11. One has to take care about the validity of low-injection lifetime measurements since the intrinsic density n_i and therefore also the electron and hole equilibrium concentrations n_0 and p_0 reach the order of the base doping at higher temperatures which is the case in our samples at temperatures of about 400K.

The high-injection lifetime, again determined by OCVD measurements, is used to calculate the electron capture coefficient (eq.12). The dependence of the capture coefficients on temperature is shown in fig.2. The comparison with the values of the electron capture coefficient calculated by means of the DLTS data show sufficient accordance within the common error limits of the DLTS measurement technique [15].

$$c_p = \frac{1}{N_T \, \tau_{LL}} \left[1 + \frac{n_i \, \exp\left(\dfrac{E_T - E_I}{k_B \, T} \right)}{n_0} \right] \tag{11}$$

$$\tau_{HL} = \tau_{n0} + \tau_{p0} = \frac{1}{c_n \cdot N_T} + \frac{1}{c_p \cdot N_T} \tag{12}$$

5.2   Electron irradiated samples

The DLTS spectrum of the electron-irradiated n-type sample E1 reveals two major peaks, the majority level E(90K) and the minority level H(195K). E(90K) corresponds to the so-called A-center, a vacancy-oxygen complex, while H(195K) originates from a carbon-oxygen complex. The minor peaks E(270K) and E(60K), known from the non-irradiated sample N and therefore not generated by irradiation, show within the accuracy of the measurement no dependency of the irradiation dose as expected.

The other electron-irradiated n-type samples show similar properties whilst the electron irradiated p-type sample gives only evidence of the levels E(90K) and H(195K). Table 3 displays the determined recombination center properties. Due to the different irradiation doses of samples E1-E3 there are different trap concentrations as shown in Table 4.

Because the different center properties only the radiation-induced center E(90K) influences the recombination behavior in a strong way, especially in case of high excess carrier concentrations, due to its high concentration and high capture cross sections. Although H(195K) is found close to midgap this level has not much influence on high-level lifetime.

However, the donor H(195K) changes the dynamic electrical behavior in semiconductor devices and should therefore be considered in device simulations [16].

Using DLTS measurements, the capture cross sections were estimated as shown in Table 5. The capture rates are calculated according to eq.10 using the values of the thermal velocities given by eq.13 and eq.14 . The capture rates of H(195K) are determined by measuring the DLTS-signal in dependence of the fill-pulse duration. The hole capture rate of E(90K) has been measured in the p-type sample by DLTS but measurements were carried out at the minimal time limit of the DLTS measurement setup which may result in a higher capture coefficient as determined here. The electron capture rate, determined from the majority carrier DLTS spectrum, is much smaller than the hole capture rate.

$$v_{TH,n} = 2.29 \cdot 10^7 \sqrt{\frac{T}{300K}} \; cm/s \qquad (13)$$

$$v_{TH,p} = 1.87 \cdot 10^7 \sqrt{\frac{T}{300K}} \; cm/s \qquad (14)$$

For device simulations of common silicon devices one needs parameters for a typical temperature range of 300-400K. In bipolar power devices such as pin-diodes, GTOs, IGBTs etc. the high-level lifetime controls forward characteristics as well as switching properties. The data for E(90K) as the dominant radiation-induced recombination center under high-injection condition are estimated by DLTS at temperatures about 90K. As shown in recent publications, these data can not be extrapolated over that wide temperature range and have to be determined by other measurements [2],[17]. Since the electron capture rate of E(90K) is much smaller than the hole capture rate, it is possible to simplify eq.12 by eliminating the second term. However, one has to consider the recombination properties of the non-irradiated sample too. Finally this results in eq.15 where τ_0 stands for the high-level lifetime in the non-irradiated silicon. The plot of the inverse high-injection lifetime τ_{HL} versus trap concentration N_T, as shown in figure 3, allows the estimation of the electron capture rate.

$$\frac{1}{\tau_{HL}} = c_n \, N_T + \frac{1}{\tau_0} \tag{15}$$

Additionally, as mentioned before in section 2.3, the validity of the measured results depends on center position and temperature. Figure 4 shows the dependence of n_1 on center position, here for E(90K) and E(270K), and on temperature.

Optical generation of free carriers by means of a laser beam results in an excess carrier concentration of about $2 \cdot 10^{17} ... 4 \cdot 10^{17} \, cm^{-3}$. Thus, in case of E(90K), the high-injection approach as the precondition of these measurements is valid for a temperature range up to app. 375K.

As the result, eq. 16 gives an approximation for the obtained electron capture rate of E(90K). In figure 5 the proposed capture rate is represented by the solid black line, whereas the solid marks are the valid measured lifetimes. The unfilled marks stand for the more inaccurate results at higher temperatures and the broken line depicts the results of common OCVD measurements based on electrical impulses, where an excess carrier concentration of $2 \cdot 10^{16} \, cm^{-3}$ is reached. This newly measured capture rate shows significantly higher values than earlier measurements in [2]. At these measurements, common OCVD was used and the lifetime of the non-irradiated silicon was not considered which both led to inaccurate results. In summary, table 6 gives the capture rates as used for device simulation.

$$c_n = 8.72 \cdot 10^{-8} \exp\left(-\frac{T}{474K}\right) cm^3 s^{-1} \tag{16}$$

6 VERIFICATION BY DEVICE SIMULATION AND COMPARISON WITH MEASUREMENTS

The structures investigated in this paper were simulated using the device simulator TeSCA [6]. It is able to solve the basic semiconductor equations for two dimensional devices or those with cylindrical symmetry. The simulator uses finite elements on a triangular mesh. It also allows some simple mixed mode simulation including several semiconductor devices.

In TeSCA, an advanced recombination model based on the Shockley-Read-Hall-statistics with full trap dynamics is used for the simulation of irradiated power diodes (Appendix B). All simulations were done with a fixed set of parameters and the trap parameters as given in table 6.

6.1 Forward Characteristics

The comparisons between the measured (symbols) and simulated (solid lines) forward characteristics for temperatures of 300K and 400K are shown in figure 6. Since the series resistance and its temperature dependence (caused by bonding wires etc.) influences the curves with increasing current, the temperature dependence of series resistance was determined and further eliminated in measurement results. Under these conditions the agreement between simulation and measurement is good even at high currents (a forward current of 30A corresponds to a current density of 500A/cm^2 or the triple nominal current).

The dependence of forward voltage on temperature is from further interest as shown in figure 7 for samples N and E3 since the knowledge of these dependencies is very important for paralleling of power devices. Generally, the recombination processes via deep traps becomes more dominant at higher currents which implies higher carrier densities. The comparison of the dependencies in figure 7 at a current of 0.3A shows an almost identical behavior of the different samples. This can be explained by the common temperature dependence of the junction voltage. At higher currents, the differences between simulation and measurement of the non-irradiated sample N is nearly identical as in sample E1 with the lowest electron

irradiation dose. With increased irradiation dose, the temperature coefficient of forward voltage $\Delta V_F/\Delta T$ is changing. The difference between simulated and measured voltage is getting smaller, indicating the growing influence of the radiation-induced recombination centers. More important, the temperature dependence of the forward voltage at a current of 30A in the simulation of sample E3 shows good accordance. The differences at the high temperatures in sample E3 are explainable by the validity of the lifetime measurements as mentioned in section 5.2.

6.2   Reverse Recovery

Reverse Recovery measurements were done using the circuit as shown in figure 8. The diode is switched from the forward conducting state to the blocking state. At the beginning of this process the middle region of the diode is assumed to be flooded with excess carriers where the exact carrier distribution is a function of the forward current density. Furthermore, the carrier distribution depends on the p- and n-emitter properties as well as on lifetime profiles.

This stored charge has to be removed during the recovery process which is either done by recombination processes or has to be swapped out as a reverse current. If carrier concentration at the pn-junction reaches the level of thermal equilibrium a space charge region is formed and the reverse current starts to decline. At this point the voltage across the diode is determined by the external circuit. In case of a significant external inductance the change in di/dt at the reverse current peak gives rise to a large spike in reverse voltage [18].

There are a number of possible solutions to minimize the stored charge and reverse voltage spikes where the use of lifetime profiles is one of the successful proved options [19]. So, for further optimization of irradiated devices it is necessary to get reliable simulation results.

As an example, figure 9 shows the simulated and measured reverse recovery waveforms of sample E3 for a temperature of 300K and 400K under the following conditions: di/dt=500A/µs, V_R=250V, I_F=10A. The good agreement between simulated and measured waveforms is found for all the samples even under different conditions. This is further

supported by the comparison of the Reverse Recovery Current Peak I_{RRM} as shown in figure 10. Due to the more exact determination of the relevant recombination center parameters the accordance of measurement and simulation results is found to be improved in comparison with earlier results [2].

Generally it is observed that the simulation allows the characterization of the device behavior in a good agreement with measurements on samples undergoing different irradiation steps.

7 CONCLUSION

The use of an extended recombination model including full trap dynamics is essential for the proper simulation of irradiated devices. Only by use of such an advanced model it is possible to consider charging processes of a relevant number of different radiation-induced recombination centers which allows a physically correct description of the recombination processes under different injection conditions. The examination of capture coefficients by means of DLTS measurements does not provide sufficient information since these parameters are strongly temperature dependent and DLTS measurements are usually performed at low temperatures. However, if it is known which recombination center does control device behavior under a certain condition, additional lifetime measurements may be used for the determination of the missing data even at high temperatures.

It is shown in this work, that high-injection lifetime at the investigated samples is controlled by the recombination center E(90K). For a reliable determination of the centers electron capture coefficient it is necessary to create a high excess carrier concentration in the devices low-doped middle region. Further, the influence of the base lifetime caused by normal silicon crystal defects and impurities has to be considered.

The introduction of the newly determined center properties into simulation leads to very satisfying results and a good accordance between measurements and simulation under varying conditions.

To further prove these results it should be necessary to vary electron irradiation energy and annealing temperature.

ACKNOWLEDGEMENTS

APPENDIX

APPENDIX A – SYMBOLS

p	hole concentration	G	generation rate
n	electron concentration	R	recombination rate
N_A	acceptor density	N_D	donor density
N_C	conduction band state density	N_V	valence band state density
N_{TA}	acceptor trap density	N_{TA}^-	ionized acceptor trap density
N_{TD}^+	ionized donor trap density	E_{TA}	acceptor trap energy level
E_T	trap energy level	f_A	fraction of occupied acceptor traps
n_i	intrinsic density	E_i	intrinsic energy level
n_0	electron equilibrium concentration	p_0	hole equilibrium concentration
δn	electron excess concentration	δp	hole excess concentration
c_n	capture rate for electrons	c_p	capture rate for holes
e_n	emission rate for electrons	e_p	emission rate for holes
χ_n	entropy factor for electrons	χ_p	entropy factor for holes
w_{SCR}	space charge region width	J_G	generation current density
τ_{n0}	electron minority carrier lifetime	τ_{p0}	hole minority carrier lifetime
V_F	forward voltage	k_B	Boltzmann's constant
q	elemental charge		

APPENDIX B – TRAP RECOMBINATION MODEL EQUATIONS

A - Poisson Equation

$$-\text{div}(\varepsilon \cdot \text{grad}\varphi) = q\left[p - n - N_A^- + N_D^+ + \Sigma\left(N_{TD}^+ - N_{TA}^-\right)\right]$$

B - Continuity Equations of Acceptors (Donors have a similar relation)

$$\frac{\partial n}{\partial t} - \text{div} J_n = G - R + \Sigma\left[e_{nA} N_{TA}^- - c_{nA} \, n\left(N_{TA} - N_{TA}^-\right)\right]$$

$$\frac{\partial p}{\partial t} + \text{div} J_p = G - R + \Sigma\left[e_{pA}\left(N_{TA} - N_{TA}^-\right) - c_{pA} \, p \, N_{TA}^-\right]$$

$$e_{nA} = \chi_{nA} c_{nA} \, n_i \, \exp\left(\frac{E_{TA} - E_I}{k_B T}\right)$$

$$e_{pA} = \chi_{pA} c_{pA} \, n_i \, \exp\left(\frac{E_I - E_{TA}}{k_B T}\right)$$

C - Probability of an Occupied State of an Acceptor (Donors have a similar relation)

$$\frac{df_A}{dt} = \left(c_{nA} \, n + e_{pA}\right)\left(1 - f_A\right) - \left(c_{pA} \, p + e_{nA}\right)f_A \qquad N_{TA}^- = N_{TA} \cdot f_A$$

APPENDIX C - HIGH-LEVEL- AND LOW-LEVEL-LIFETIME FOR A SINGLE RECOMBINATION CENTER

A - Shockley-Read-Hall-Recombination rate and lifetime

From eq.1 and with $n=n_0+\delta p$ one obtains:

$$R = \frac{\delta n\, p_0 + \delta p\, n_0 + \delta n\, \delta p}{\tau_{p0}\left[n_0 + \delta n + N_C \exp\left(\dfrac{E_T - E_C}{k_B T}\right)\right] + \tau_{n0}\left[p_0 + \delta p + N_V \exp\left(\dfrac{E_V - E_T}{k_B T}\right)\right]}$$

$$\delta n = \delta p$$

$$\tau = \frac{\delta n}{R} = \tau_{p0}\left[\frac{n_0 + \delta n + N_C \exp\left(\dfrac{E_T - E_C}{k_B T}\right)}{n_0 + p_0 + \delta n}\right] + \tau_{n0}\left[\frac{p_0 + \delta n + N_V \exp\left(\dfrac{E_V - E_T}{k_B T}\right)}{n_0 + p_0 + \delta n}\right]$$

$$\tau_{n0} = \frac{1}{c_n \cdot N_T} \qquad\qquad \tau_{p0} = \frac{1}{c_p \cdot N_T}$$

B - Low-level lifetime

$n_0 \gg \delta n$, $n_0 \gg p_0$ (n-type silicon)

$$\tau_{LL} = \tau_{p0}\left[1 + \exp\left(\frac{E_T - E_F}{k_B T}\right)\right] + \tau_{n0}\exp\left[\frac{2E_I - E_T - E_F}{k_B T}\right]$$

C - High-level lifetime

$$\delta n \gg n_0, n_1, p_0, p_1$$

$$n_1 = n_i \exp\left(\frac{E_T - E_I}{k_B T}\right)$$

$$\tau_{HL} = \tau_{n0} + \tau_{p0}$$

REFERENCES

1. J.Vobecký, P.Hazdra, J.Voves. Accurate Simulation of Combined Electron and Ion Irradiated Silicon Devices for Local Lifetime Tailoring, Proc. ISPSD, pp.265-270, 1994

2. R.Siemieniec, D.Schipanski, W.Südkamp, J.Lutz. Simulation and Experimental Results of Irradiated Power Diodes, Proc. EPE 1999, Lausanne

3. W.Shockley, W.T.Read. Statistics of the recombinations of holes and electrons, Physical Review, Vol.87, No.5, pp.835-842, September 1952

4. R.N.Hall. Electron-Hole Recombination in Germanium, Physical Review, Vol.87, No.2, p.387, July 1952

5. P.Mourick. Das Abschaltverhalten von Leistungsdioden, Dissertation, TU Berlin, 1988

6. H.Gajewski et al, TeSCA Manual, Berlin, 1991-1999

7. D.V.Lang. Deep-level transient spectroscopy: A new method to characterize traps in semiconductors. Journal of Applied Physics 1974; 45 (7): p.3023-3032

8. Lederhandler S.R., Giacoletto L.J.. Measurement of Minority Carrier Lifetime and Surface Effects in Junction Devices. Proceedings IRE, 1955, p.477-483

9. Jain S.C., Muralidharan R., Effect of Emitter Recombination on the Open Circuit Voltage Decay of a Junction Diode. Solid-State Electronics, Vol.24, pp. 1147-1154, 1981,

10. Basset R.J., Fulop W., Hogarth C.A. Determination of the bulk carrier lifetime in the low-doped region of a silicon power diode, by the method of open circuit voltage decay. Int. J. Electronics, 1973, 35 (2), p.177-192

11. M.A.Green. Minority Carrier Lifetimes Using Compensated Differential Open Circuit Voltage Decay. Solid-State Electronics, Vol.26, No.11, pp.1117-1122, 1983

12. V.Grivickas. An accurate method for determining intrinsic optical absorption in indirect band gap semiconductors, Solid State Communications, Vol.108, No.8, pp.561-566, 1998

13. S.Gall. Admittanzspektroskopische Untersuchungen des a-SiH/c-Si-Heteroüberganges im Hinblick auf photovoltaische Anwendungen, Dissertation, TU Berlin, 1997

14. JOL-R60 - Gütegeschalteter diodengepumpter Festkörperlaser, Spezifikation, JENOPTIK Geschäftsbereich Lasertechnik, Jena

15. W.Wondrak. Erzeugung von Strahlenschäden in Silizium durch hochenergetische Elektronen und Protonen, Dissertation, Universität Frankfurt/Main, pp. 70-73, 1985

16. J.Lutz, W.Südkamp, W.Gerlach. Impatt Oscillations in Fast Recovery Diodes due to Temporarily Charged Radiation-Induced Deep Levels, Solid-State Electronics, Vol.42, No.6, pp.931-938, 1998

17. H.Bleichner, P.Jonsson, N.Keskitalo, E.Nordlander. Temperature and injection dependence of the Shockley-Read-Hall Lifetime in electron irradiated n-type silicon, Journal of Applied Physics 79 (12), pp.9142, June 1996

18. V.Benda, J.Gowar, D.A.Grant. Power Semiconductor Devices, John Wiley & Sons, 1999

19. J. Lutz. Axial Recombination Center Technology for Freewheeling Diodes. Proceedings EPE, Trondheim, 1997

TABLES:

TABLE 1: Sample Overview

Sample	Type	Irradiation	Dose
N	n-Si	none	-
E1	n-Si	Electron	10%
E2	n-Si	Electron	50%
E3	n-Si	Electron	100%
PE	p-Si	Electron	10%

TABLE 2: Parameters of recombination centers in Sample N determined by DLTS measurements

Signal	N_T [cm^{-3}]	E_V+E_T [eV]	σ_0 [cm^2]	E_σ [meV]	$c_{n,p}$ (300K) [cm^3/s]	τ (300K) [μs]
E(270K)$_{slow}$ (c_n)	$5.7 \cdot 10^{10}$	0.578	$8.44 \cdot 10^{-16}$	-41.18	$3.93 \cdot 10^{-9}$	4460
E(270K)$_{fast}$ (c_n)	$3.0 \cdot 10^{10}$	0.578	$1.17 \cdot 10^{-14}$	38.33	$1.18 \cdot 10^{-6}$	28.2
H(260K) (c_p)	$7.4 \cdot 10^{11}$	0.42	$7.08 \cdot 10^{-18}$	35.96	$5.32 \cdot 10^{-10}$	2540
H(170K) (c_n)	$7.1 \cdot 10^{10}$	0.357	$1.48 \cdot 10^{-15}$	19.51	$7.19 \cdot 10^{-8}$	196
E(60K)	$9.5 \cdot 10^{11}$	1.003	-	-	-	-

TABLE 3: Parameters of recombination centers in electron irradiated samples as estimated by DLTS measurements

Signal	Sample	E_V+E_T [eV]	σ [cm^2]	T at 100/s [K]
E(60K)	E1 (n)	1.003	$7.18 \cdot 10^{-15}$	63
E(90K)	E1 (n)	0.953	$3.01 \cdot 10^{-15}$	91
E(90K)	PE (p)	0.953	$2.94 \cdot 10^{-15}$	91
E(270K)	E1 (n)	0.578	$1.78 \cdot 10^{-15}$	275
H(195K)	E1 (n)	0.356	$1.21 \cdot 10^{-15}$	199
H(195K)	PE (p)	0.355	$9.11 \cdot 10^{-16}$	199

TABLE 4: Recombination center concentration in dependence of irradiation dose

Sample	Dose	E(60K)	E(90K)	E(270K)	H(195K)
E1	10%	$1.88 \cdot 10^{12}$ cm^{-3}	$4.16 \cdot 10^{12}$ cm^{-3}	$1.8 \cdot 10^{11}$ cm^{-3}	$5.2 \cdot 10^{12}$ cm^{-3}
E2	50%	$2.26 \cdot 10^{12}$ cm^{-3}	$2.47 \cdot 10^{13}$ cm^{-3}	$2.02 \cdot 10^{11}$ cm^{-3}	$2.75 \cdot 10^{13}$ cm^{-3}
E3	100%	$2.96 \cdot 10^{12}$ cm^{-3}	$3.29 \cdot 10^{13}$ cm^{-3}	-	$5.51 \cdot 10^{13}$ cm^{-3}

TABLE 5: Complete trap parameters of the relevant radiation-induced centers determined by DLTS measurements

Trap	σ_n [cm^2]	$E_{\sigma n}$ [eV]	χ_n	σ_p [cm^2]	$E_{\sigma p}$ [eV]	χ_p
E(90K)	$7.68\cdot10^{-15}$	$3.64\cdot10^{-3}$	0.54	$3.42\cdot10^{-14}$	$6.15\cdot10^{-3}$	1.85
H(195K)	$4.3\cdot10^{-16}$	$-8.5\cdot10^{-2}$	0.25	$2.3\cdot10^{-16}$	0	3.96

TABLE 6: Capture rates of the recombination centers used in device simulation

Trap	Electron capture rate c_n [cm^3/s]	Hole capture rate c_p [cm^3/s]
E(270K)	$4.98\cdot10^{-6}\,\exp\!\left(-3.66\cdot10^{-3}\,\mathrm{K}^{-1}\cdot T\right)$	$4.58\cdot10^{-10}\,\exp\!\left(3.2\cdot10^{-2}\,\mathrm{K}^{-1}\cdot T\right)$
E(90K)	$8.72\cdot10^{-8}\,\exp\!\left(-\dfrac{T}{474\mathrm{K}}\right)$	$6.39\cdot10^{-7}\,\sqrt{\dfrac{T}{300\mathrm{K}}}\,\exp\!\left(\dfrac{6.15\cdot10^{-3}\,\mathrm{eV\,K}}{k_B T}\right)$
H(195K)	$9.85\cdot10^{-9}\,\sqrt{\dfrac{T}{300\mathrm{K}}}\,\exp\!\left(-\dfrac{85\cdot10^{-3}\,\mathrm{eV\,K}}{k_B T}\right)$	$4.3\cdot10^{-9}\,\sqrt{\dfrac{T}{300\mathrm{K}}}$

FIGURES:
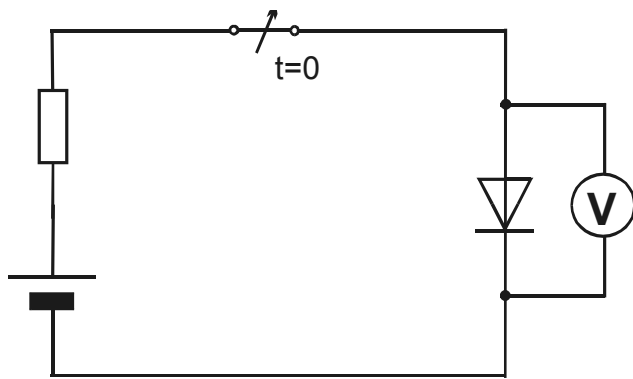
Fig.1a: OCVD schematic
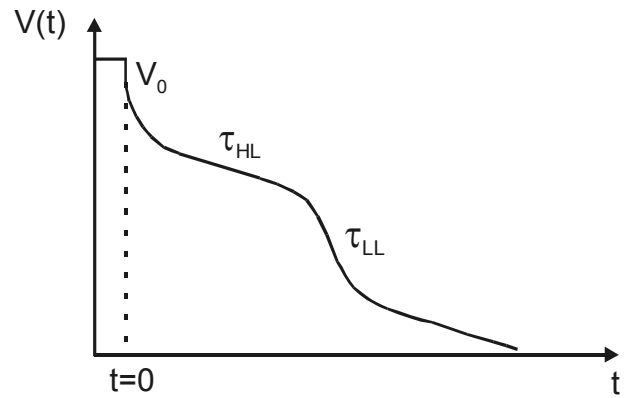
Fig. 1b: OCVD voltage waveform
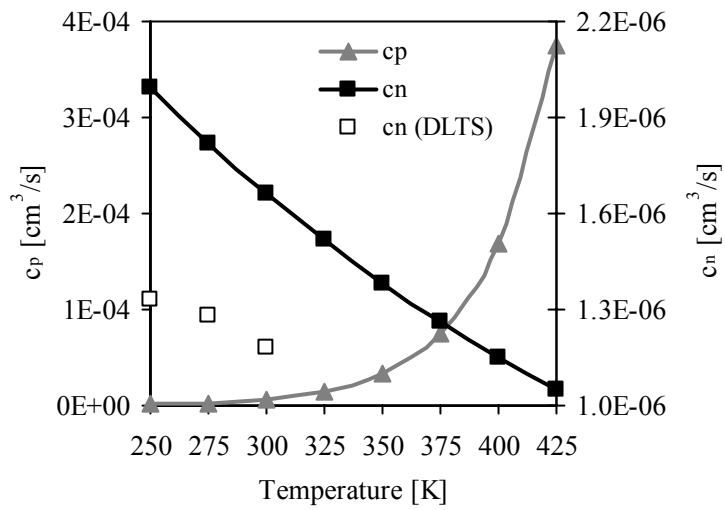
Fig. 2: Capture Coefficients of E(270K)
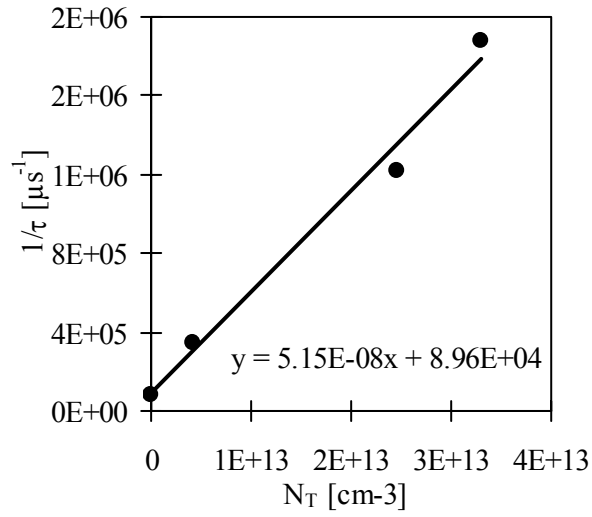
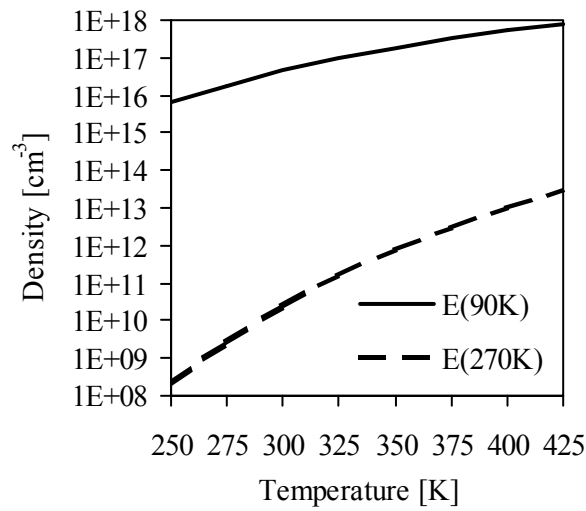Fig. 3: Estimation of the electron capture rate (T=250K)

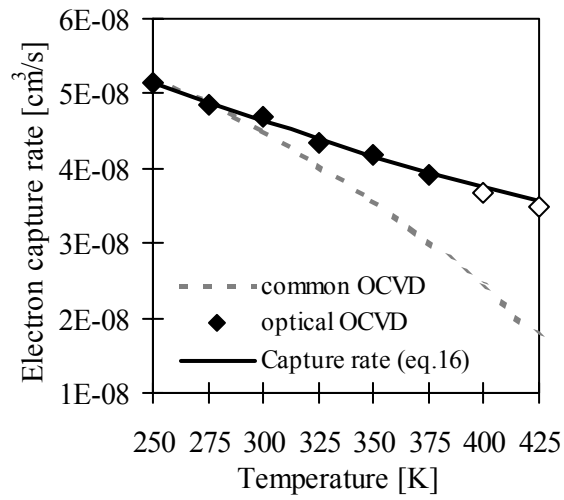Fig. 4: Dependence of n_1 on temperature and trap position
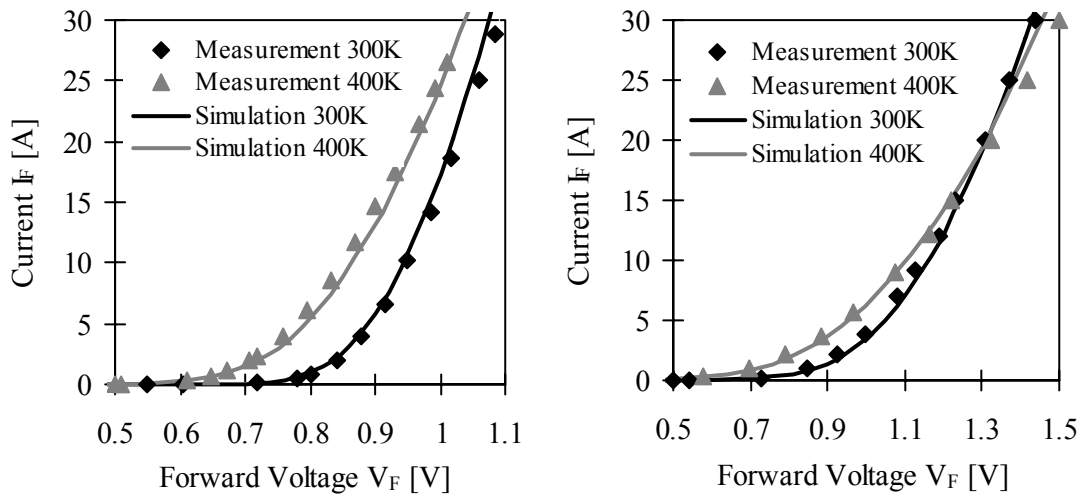
Fig. 5: Measured electron capture rate of E(90K)

Fig. 6: Measured and simulated forward characteristics of samples N (left) and E3 (right)
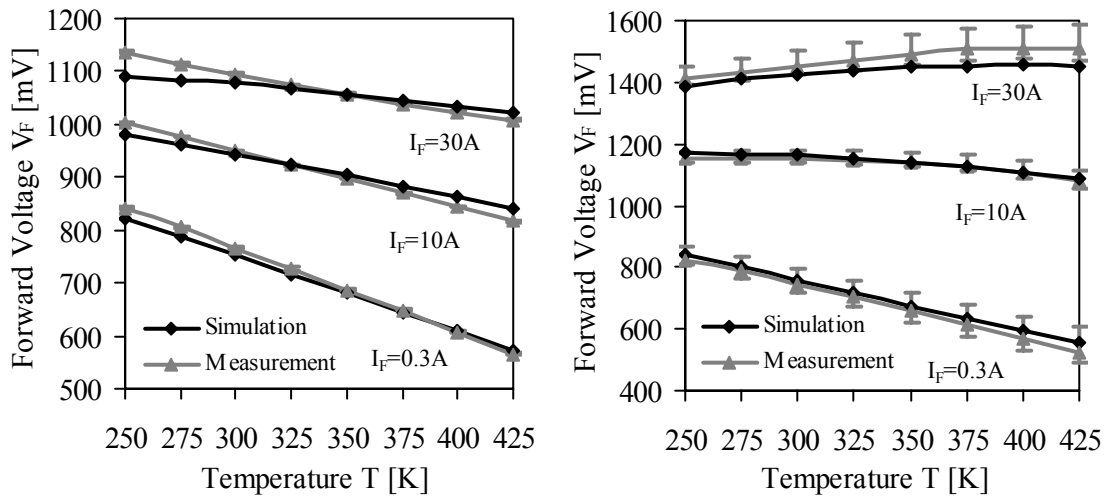
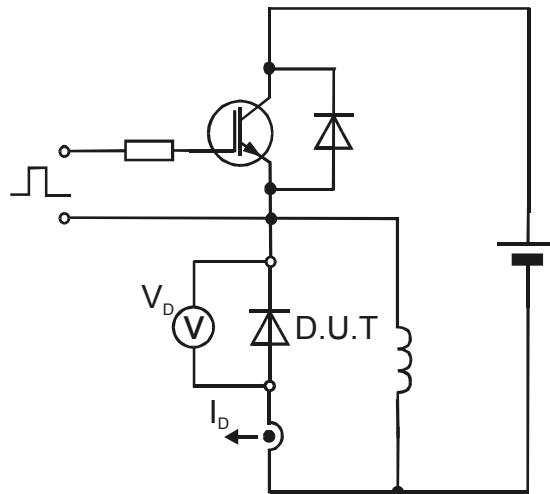Fig. 7: Forward voltage dependence on temperature of samples N (left) and E3 (right)

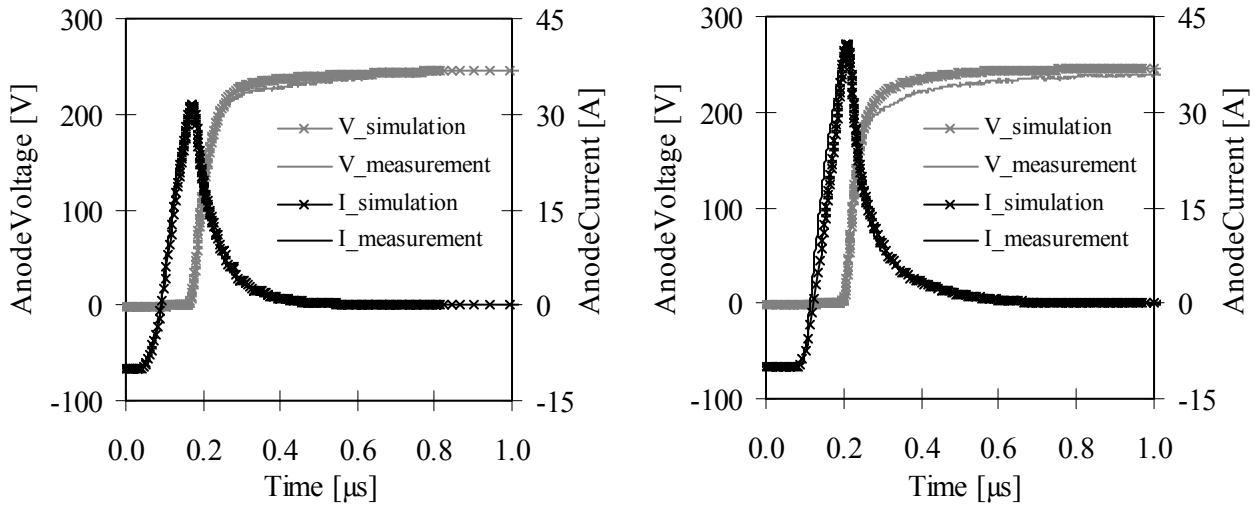

Fig. 8: Reverse Recovery measurement setup

Fig. 9: Reverse Recovery of sample E3 at T=300K (left) and T=400K (right)
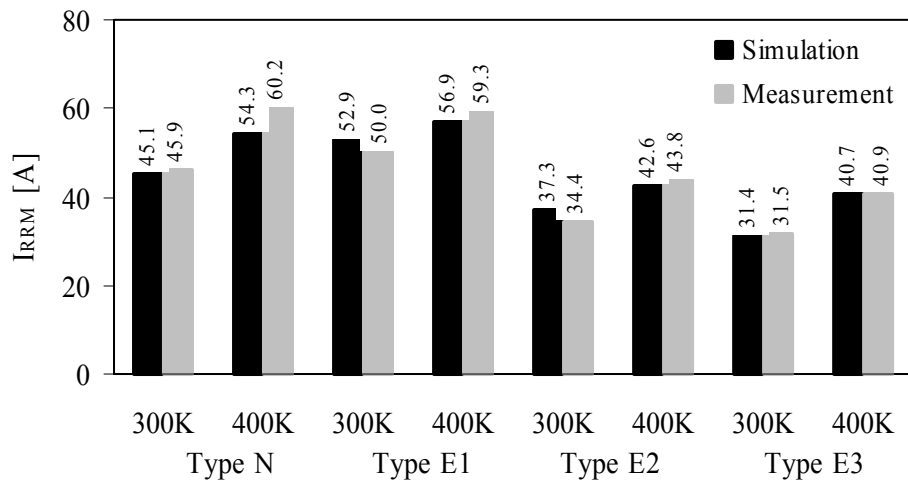

Fig. 10: Comparison of I_{RRM} for the different samples at 10A and 500A/µs